Graphene oxide directed in-situ synthesis of Prussian blue for non-enzymatic sensing of hydrogen peroxide released from macrophages

Weiwei Qiu [a], Qionghua Zhu [a], Fei Gao [a], Feng Gao [a], Jiafu Huang [b], Yutian Pan [b], Qingxiang Wang [a,*]

[a] College of Chemistry and Environment, Fujian Province Key Laboratory of Morden Analytical Science and Separation Technology, Minnan Normal University, Zhangzhou 363000, PR China
[b] College of Biological Science and Technology, Minnan Normal University, Zhangzhou 363000, PR China

ARTICLE INFO

ABSTRACT

A novel electrochemical non-enzymatic hydrogen peroxide (H_2O_2) sensor has been developed based on Prussian blue (PB) and electrochemically reduced graphene oxide (ERGO). The GO was covalently modified on glassy carbon electrode (GCE), and utilized as a directing platform for in-situ synthesis of electroactive PB. Then the GO was electrochemically treated to reduction form to improve the effective surface area and electroactivity of the sensing interface. The fabrication process was characterized by scanning electron microscopy (SEM), energy-dispersive X-ray spectroscopy (EDX) and atomic force microscopy (AFM). The results showed that the rich oxygen containing groups play a crucial role for the successful synthesis of PB, and the obtained PB layer on the covalently immobilized GO has good stability. Electrochemical sensing assay showed that the modified electrode had tremendous electrocatalytic property for the reduction of H_2O_2. The steady-state current response increased linearly with H_2O_2 concentrations from 5 μM to 1 mM with a fast response time (less than 3 s). The detection limit was estimated to be 0.8 μM. When the sensor was applied for determination of H_2O_2 released from living cells of macrophages, satisfactory results were achieved.

© 2016 Elsevier B.V. All rights reserved.

1. Introduction

Hydrogen peroxide (H_2O_2), as a common molecule in nature, shows widespread applications in pharmaceutical, clinic, environmental, mining, textile, paper, food manufacturing and chemical industries [1]. In biological field, it has been reported that the concentration level of H_2O_2 is an essential biological parameter in monitoring and maintaining the physiological balance of living cells, and the abnormal concentration level of H_2O_2 in body will lead to cell aberrance and apotosis, causing different kinds of diseases, such as Parkinson's, Alzheimer's, cancer, diabetes, cardiovascular and neurodegenerative disorders [2,3]. Therefore, the development of highly sensitive, accurate, rapid and economical method for the determination of H_2O_2, especially released from living cells is of utmost importance in both biomedical and environmental studies [4–6]. Due to the intrinsic simplicity, rapidness, high sensitivity and selectivity, low cost, electrochemical method has been extensively employed in H_2O_2 sensor design and construction [7–9]. The enzyme-based electrochemical H_2O_2 sensors exhibit outstanding advantages of high sensitivity and high selectivity, but their utility is usually debased by the prohibitive costs of enzymes, complicated electrode fabrication process, poor stability, and harsh condition of test. Alternatively, non-

enzymatic H_2O_2 sensors on the basis of nanomaterials are good candidates for robust detection of H_2O_2 due to their high stability, abundant active sites, excellent catalytic activity [10,11]. Up to now, numerous nanomaterials have been successfully used for the fabrication of non-enzymatic H_2O_2 sensors, such as noble metals, metal oxides, and carbonaceous materials [5,12–15]. But the high price and complicated synthesis procedures these materials restrains their practical application.

Prussian blue (PB) is a typical inorganic material, which shows extensive application in various fields such as capacitor material, electrochromic devices, catalysis, medicines, and so on [16]. PB has also been denoted as an "artificial peroxidase" because of its catalytic effect toward many biological important molecules such as cholesterol [17] and glucoses [18]. In addition, due to its excellent electroactivity, high selectivity and porous structure, PB or its composite has also been utilized as redox mediator in H_2O_2 biosensor construction [19,20].

The fabrication of PB-based biosensors can be commonly accomplished by direct electrosynthesis [21] or physical coating coupled with chemical pre-synthesis [22]. The electrodeposition of PB on the electrode surface is convenient and thickness controllable, but the too fast growth process of PB arising from its ultralow solubility product constant ($K_{sp} = 3.3 \times 10^{-41}$) makes the morphology and size of the electrosynthesised product hard to be controlled. PB synthesized through homogeneous chemical method also has above mentioned disadvantages, and meanwhile the modification process of the pre-

* Corresponding author.
E-mail address: axiang236@126.com (Q. Wang).

synthesized PB on solid electrode surface is complicated. In addition to this, some film-forming reagent or binders are necessary, which will cause inferior electronic conductivity as well as the low sensitivity of the sensors.

In contrast, the in-situ self-assembly method based on successive adsorptions of Fe^{3+} and $Fe(CN)_6^{4-}$ on an appropriate matrix to synthesize PB not only can effectively control the growth rate as well as uniformity and morphology of PB, but also can greatly enhance its physicochemical properties such as mechanical strength and chemical stability [23]. Based on these merits, Manivannan et al. [24] used amine-functionalized silicate sol-gel reduced graphene oxide composite as the matrix for the in-situ synthesis of PB, leading to a three-dimension cage-like porous nanostructure. Electrochemical experiment showed that the unique electron-transfer mediating process of PB integrated with highly conductive reduced graphene oxide synthesized via the in-situ assembly method facilitated synergistic electrocatalytic activity for methanol oxidation. Ojani et al. [25] also synthesized PB through in-situ assembly method on a poly (o-phenylenediamine) modified electrode, which was utilized as an electrochemical sensor for H_2O_2 in acid media. However, in order to successfully obtain the in-situ synthesized PB, a non-conductive supporting matrix such as amine-functionalized silicate sol-gel [24] or poly (o-phenylenediamine) [25] was used, which not only increased fabrication cost and procedure, but also decreased the electrochemical activity of PB.

In order to overcome these disadvantages that happened in the conventional synthesis method of PB, the graphene oxide (GO) with rich functional groups was used as a directing platform for in-situ synthesis of PB in this work. The GO was first immobilized on a glassy carbon electrode (GCE) via a covalent bonding method, then the PB was grown on GO through sequential dipping in Fe^{3+} and $Fe(CN)_6^{4-}$ solutions. Characterization experiments suggested that the functional oxygen-containing groups were crucial for the GO-directed growth of PB. Then in order to improve the electroactivity of the synthesized PB, the modified electrode was electrochemically treated to transfer GO film to the reduced form (ERGO), which was more convenient and safe than the traditional chemical reduction methods [26,27]. So, the proposed method that combines in-situ growth of PB and direct electro-reduction of GO presented the advantages of higher stability, easier fabrication process and better analytical performance. Electrochemical analytical results showed that the prepared electrode could been utilized as a robust sensor for electrochemical analysis of H_2O_2 with wide linear range, fast response rate and excellent anti-interference ability. Based on these features, the electrode was applied as an electrochemical sensor for the effective monitoring of H_2O_2 released from living cells.

2. Experimental

2.1. Reagents and apparatus

Graphite and ascorbic acid (AA) of analytical grade were obtained from Guangdong Xilong Chemical Co., Ltd. (China). Dopamine (DA) was acquired from Aladdin Reagent Co., Ltd. (China). H_2O_2 and glucose (Glu) were provided by Hengmao Chemical Reagent Co., Ltd. (China). Lipopolysaccharide (LPS) and catalase were obtained from Sigma-Aldrich (China). N-Hydroxy succinimide (NHS), 1-(3-dimethylaminopropyl)-3-ethylcarbodiimide hydrochloride (EDC), potassium ferrocyanide ($K_4Fe(CN)_6$) and ferric chloride hexahydrate ($FeCl_3 \cdot 6H_2O$) were purchased from Shanghai Jingchun Reagent Co., Ltd. (China). The macrophages were provided by BeNa Culture Collection Co., Ltd. (China). Uric acid (UA) was supplied by Sangon Bioengineering Co., Ltd. (China). Nafion was obtained from Shanghai New-energy Technology Co., Ltd. (China). All the other chemicals were of analytical reagent grade and obtained commercially. Doubly distilled water was used throughout the experiments.

Morphology of the modified electrode was recorded on JEOL JSM-5600F Field-Emission Scanning Electron Microscopy (SEM, Japan).

Atomic force microscopy (AFM) measurements were carried out on CSPM5500 scanning probe microscope (China). The pH values were tested on a model pHS-25 digital acidometer (China). Electrochemical measurements were measured by a CHI 650C electrochemical analyzer (China) with a conventional three-electrode system composed of Pt wire as auxiliary, Ag/AgCl electrode as the reference electrode, and a glassy carbon electrode (GCE, $\Phi = 3$ mm) modified with different materials as the working electrode. The SEM and AFM characterization on the morphology of the electrode were performed on a detachable working electrode purchased from Gaoss Union Tech. Co., Ltd. (China).

2.2. Covalent immobilization of GO on GCE

Prior modification, the bare GCE was polished to a mirror-like surface with 1.0, 0.3, and 0.05 μm α-Al_2O_3, followed by ultrasonic rinsing with water, ethanol-water mixture (V/V = 1:1), and water in turn. Then the electrode was dried under a high-purity N_2 stream. GO was synthesized from graphite powder according to Hummer's method [28]. The homogeneous GO suspension (1.0 mg mL^{-1}) was prepared by dispersing 5 mg GO in 5 mL water with ultrasonication for 5 h. The fabrication procedure of the sensor was illustrated in Scheme 1. In detail, the cleaned electrode was oxidized at $+0.5$ V for 60 s in 0.05 M PBS (pH 7.0) to generate oxygen-containing functional groups on the electrode surface [29]. Then the oxidized GCE was activated in 200 μL mixture solution containing 5.0 mM EDC and 8.0 mM NHS for 2 h, followed by rinsing with water. Afterward, 10 μL of prepared GO suspension was dropped onto the activated GCE surface and dried in air. After sufficiently washed with water to remove the loosely absorbed GO, the GO covalently modified GCE (GO/GCE) was prepared.

2.3. In-situ growth of PB on GO/GCE and the electro-reduction treatment

For the in-situ growth of PB on GO/GCE, the GO/GCE was subsequently immersed in Solution A (0.01 M $FeCl_3$, 0.1 M HCl and 0.1 M KCl) for 1 min, water for 30 s, Solution B (0.01 M $K_4[Fe(CN)_6]$, 0.1 M KCl) for 1 min, and water for 30 s at 37 °C. Such a dipping process was repeated for 10 times to make sure of adequate growth of PB nanoparticles on GO/GCE. The obtained electrode was denoted as PB-GO/GCE. Afterwards, the PB-GO/GCE was immersed into 0.05 M PBS (pH 7.0), and cyclically swept within a potential range of -1.6–0.6 V at 50 mV s^{-1} to transform GO to the reduced form (ERGO) [30]. The obtained electrode was denoted as PB-ERGO/GCE. Finally, in order to improve selectivity and stability of the prepared electrode, 5 μL 0.5% Nafion was cast on the PB-ERGO/GCE surface. After dryness and washed with water, the sensor (Nafion/PB-ERGO/GCE) was achieved.

In addition, in order to probe whether PB was grown specifically on GO modified electrode, an electrode of GO/GCE was electro-reduced first, and then used as the directing platform for growth of PB. The obtained control electrode was named as PB-pERGO/GCE. Also, in order to investigate sensing performance of each constitute in the sensing film, the electrodes of GO/GCE and PB-GO/GCE were fabricated through the same procedures.

3. Results and discussion

3.1. Morphologic and structure characterization

The appropriate matrix with functional groups is very attractive as support and stabilizer for the nanoparticles in both solution and solid phase [31]. In this work, the GO with rich functional groups of —COOH, —OH, and epoxy that covalently anchored on GCE was utilized as solid-phase support for the in-situ growth of PB particles. The growth process was characterized by SEM, and the results were displayed in Fig. 1. As seen, the bare GCE showed a flat and smooth surface (Fig. 1A). Upon modification of GCE with GO, some corrugated regions (Fig. 1B, see the arrow) that was consistent with the characteristic of GO was
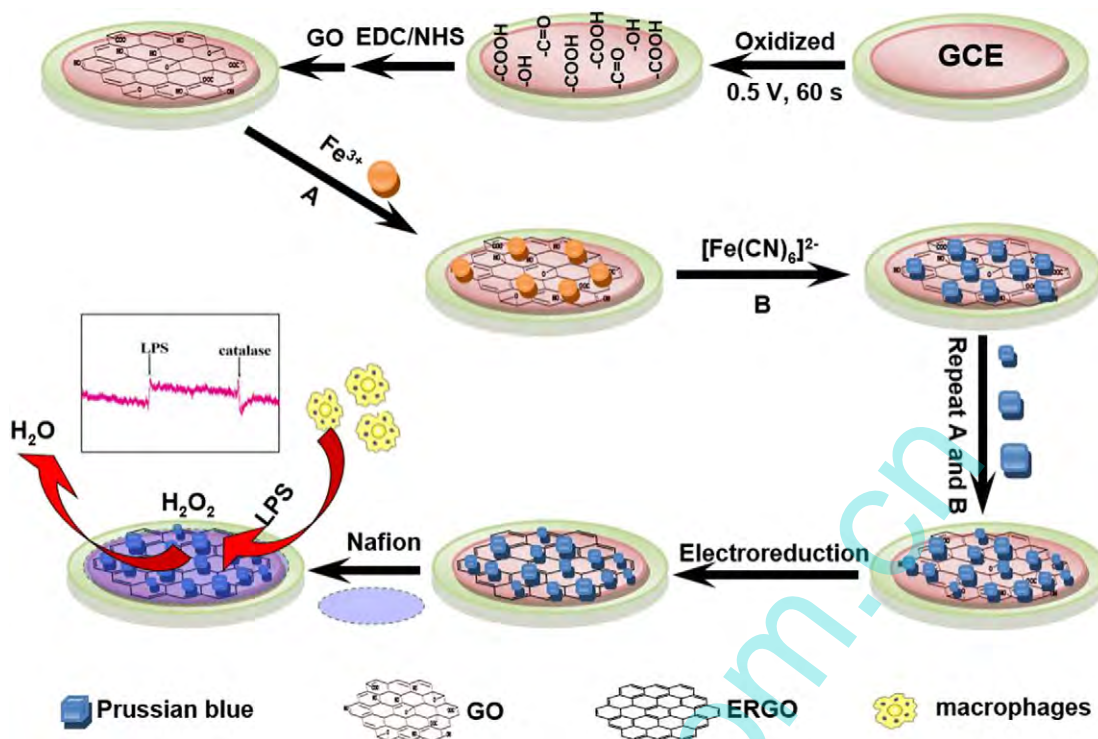
Scheme 1. Illustration for the fabrication and electrochemical sensing application of Nafion/PB-ERGO modified electrode.

observed, suggesting that the GO had been successfully confined on the electrode surface. After the GO/GCE was subsequently immersed in Solution A and Solution B as described in experimental section, it was clearly found that some cubic particles were dispersed on the surface of the GO/GCE, and the diameter of the obtained particles were in the range from 100 nm to 400 nm (Fig. 1C).

The EDX analysis demonstrated that the particles were comprised by the elements of Fe, N, C and K (Fig. 1a), confirming that PB had grown on the surface of GO. In order to probe the effect of the functional groups of GO on the in-situ growth of PB, the pre-electroreduced electrode of GO/GCE, i.e., pERGO/GCE was also applied as supporting matrix to successively dipping in Solution A and Solution B. Interestingly, the SEM image (Fig. 1D) showed that only a few PB particles were observed, and the EDX analysis (Fig. 1b) confirmed the few particles were PB. Therefore, it could be concluded that the oxygen-containing functional groups play a crucial role for the in-situ large-scale synthesis of PB.

The growth mechanism could be proposed as a "reactive self-assembly process" [32]: when GO/GCE was immersed into Solution A, the hydrophilicity of GO facilitate the permeation and adsorption of Fe^{3+} cations on the GO surface via the electrostatic and/or coordinative interaction with the negatively charged oxygenic groups. Then the electrode was immersed into Solution B, the adsorbed Fe^{3+} cations further react with the $[Fe(CN)_6]^{4-}$ anion, and form the insoluble crystal nucleus of $Fe_x[Fe(CN)_6]_y$ on the surface of GO. After repetitive dipping in Solution A and Solution B, the crystal nucleus of $Fe_x[Fe(CN)_6]_y$ continuously grow, and finally form PB nanoparticle layer on the electrode surface.

Atomic force microscopy (AFM) is a high-resolution scanning probe microscopy, which can be conducted to probe the topography changes of an interface. The formation of PB on the GO modified electrode was further characterized by AFM. Fig. 2 showed the three-dimension (3D) (curve a), topographic (curve b), and cross-sectional (curve c) AFM images of bare GCE (A), GO/GCE (B), PB-GO/GCE (C) and PB-pERGO/GCE (D). As seen, the surface of bare GCE was flat and smooth. The largest height and the average roughness degree (R) that calculated from

different regions were determined to 1.83 nm and 1.27 nm, respectively. However, when GO was covalently immobilized on GCE, the flat electrode surface was transformed to mountain chain-like peaks. The largest height and average roughness were raised to 4.26 nm and 2.65 nm, respectively, suggesting that GO had been grafted on the electrode surface. After PB particles were further grew on the surface of GO/GCE, the AFM results changed dramatically. It was observed that lots of hill-like peaks appeared, and the largest peak height and the roughness were evidently increased to 42.01 and 38.22 nm, respectively, confirming that the PB nanoparticles had been successfully prepared on GO modified electrode through the proposed approach. For comparison, the AFM result of PB formed on pERGO/GCE was also recorded, and the result revealed that the surface of this electrode was very different with that of PB-GO/GCE, but was similar with that of GO/GCE. The height and the average roughness were only 8.45 and 5.81 nm, respectively. This result further testified that only few of PB was formed on pERGO/GCE, likely due to the lack of active groups on pERGO for the effective growth of PB. These results also indicated that GO was capable of acting as an effective directing platform for the in-situ synthesis of PB.

3.2. Electrochemical behaviors of PB modified electrode

Fig. 3A showed the corresponding CVs of (a) GO/GCE, (b) PB-GO/GCE and (c) PB-ERGO/GCE within the potential range from −0.8 to 0.6 V in 0.1 M KCl (pH = 2.0). As seen, not any Faradic response was observed on GO/GCE, suggesting that the modified layer of GO was electro-inactive under the test conditions. However, after the electrode was deposited with the PB via the proposed in-situ growth method, a pair of well-defined redox peak was observed at +0.116 V and +0.220 V with the anodic peak currents (I_{pa}) of −30.7 μA and the cathodic peak currents (I_{pc}) of 98.2 μA. The redox peak potentials were in good consistence with those of PB in literature [33,34]. Upon further electrochemical treatment in 0.05 M PBS buffer to transfer GO layer to the reduced form of ERGO, it was found that the background currents
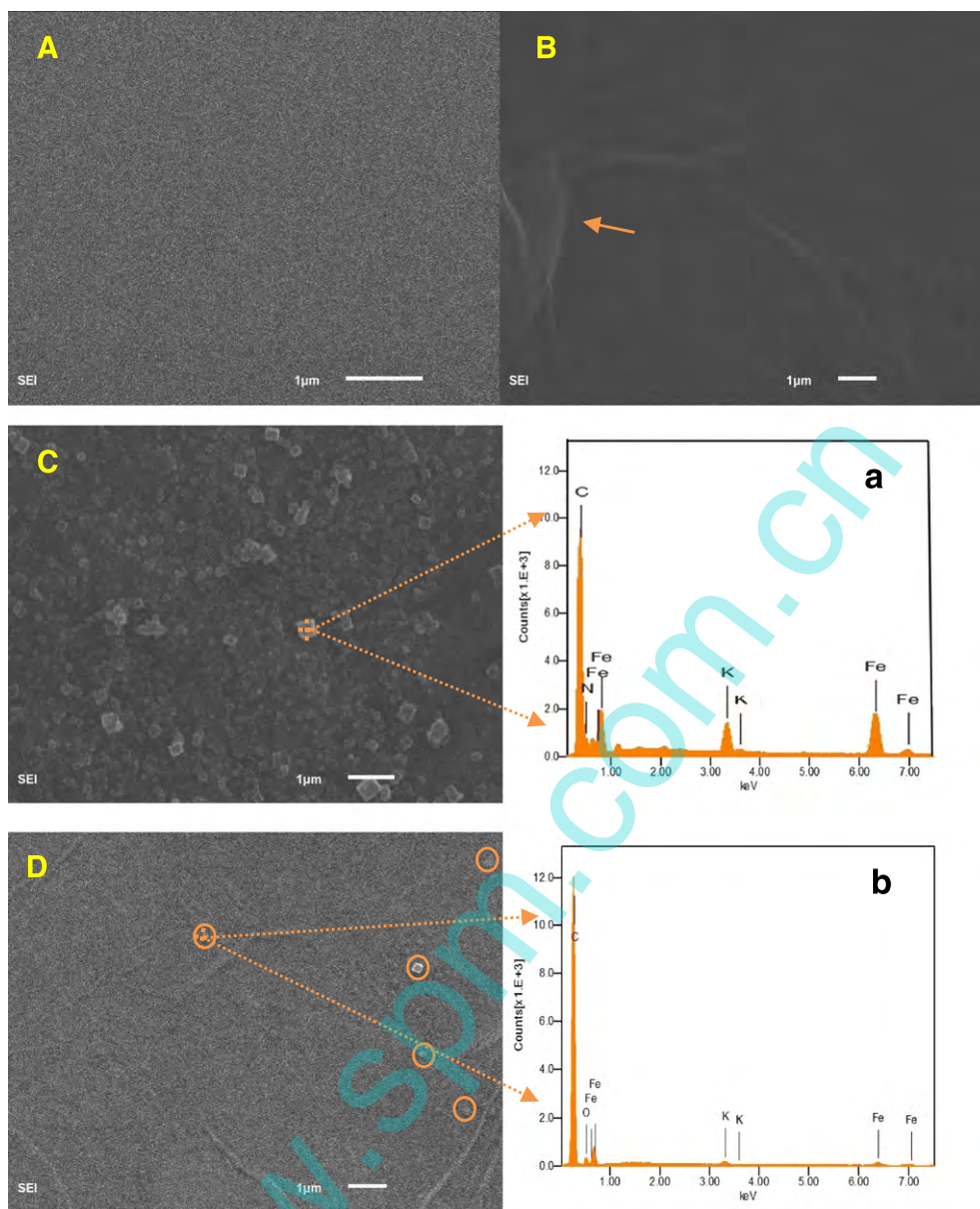
Fig. 1. SEM images of GCE (A), GO/GCE (B), PB-GO/GCE (C) and PB-pERGO/GCE (D), and EDX patterns of PB-GO/GCE (a) and PB-pERGO/GCE (b). The SEM and EDX results for PB-GO/GCE and PB-pERGO/GCE were obtained after immersing in Fe^{3+} and $[Fe(CN)_6]^{4-}$ solutions for 10 cycles.

of the electrode increased significantly (curve c), and meanwhile, the I_{pa} and I_{pc} were respectively increased to -160.7 μA and 253.5 μA. The ratio of I_{pa}/I_{pc} was much closer to one unit in comparison with the un-reduced one. These results demonstrated that GO layer had been well reduced, which increased the effective surface area of the electrode and electron transfer reversibility of the electroactive materials.

Furthermore, the electrochemical behaviors of PB-ERGO/GCE at various scan rates (v) were examined, and the results were displayed in Fig. 3B. It was observed that both the reduction peaks and the oxidation peaks enhanced with the increase of scan rate, and the peak currents (I_{pc}) showed good linear relationships with the square root of scan rate ($v^{1/2}$), obeying the regression equations of I_{pa} $(10^{-6}A) = 105.2 - 2150\ v^{1/2}$ $(V^{1/2}/s^{1/2})$ $(R = 0.999)$ and I_{pc} $(10^{-6}A) = 18.49 + 2230\ v^{1/2}$ $(V^{1/2}/s^{1/2})$ $(R = 0.998)$, respectively (Fig. 3C). The results indicated that the electron transfer reaction of PB on the electrode surface was controlled by a diffusion process [35], which could be explained by the fact that the electrochemical reaction process of PB was

accompanied by the diffusion of K^+ from bulk solution to the electrode surface as displayed in the following equation:

$$KFe^{III}\left[Fe^{II}(CN)_6\right]\ (electrode)+K^+(solution)+e^-\rightleftharpoons K_2Fe^{II}\left[Fe^{II}(CN)_6\right] \quad (1)$$
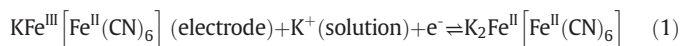
3.3. Electrocatalytic activity toward the reduction of H_2O_2

To probe the potential application of the fabricated PB/ERGO/GCE, it was applied as an electrochemical sensor for the catalytic analysis of H_2O_2. It was of note that in order to enhance the stability and anti-interference of the sensor, a layer of Nafion was utilized to cast on the PB-modified electrode surface. Fig. 4 showed the CVs of Nafion/ERGO/GCE (A), Nafion/PB-GO/GCE (B), and Nafion/PB-ERGO/GCE (C) in N_2-saturated electrolyte without (curve a) and with (curve b) 1.0 mM H_2O_2. It was observed that the CVs of ERGO/GCE in absence and presence of
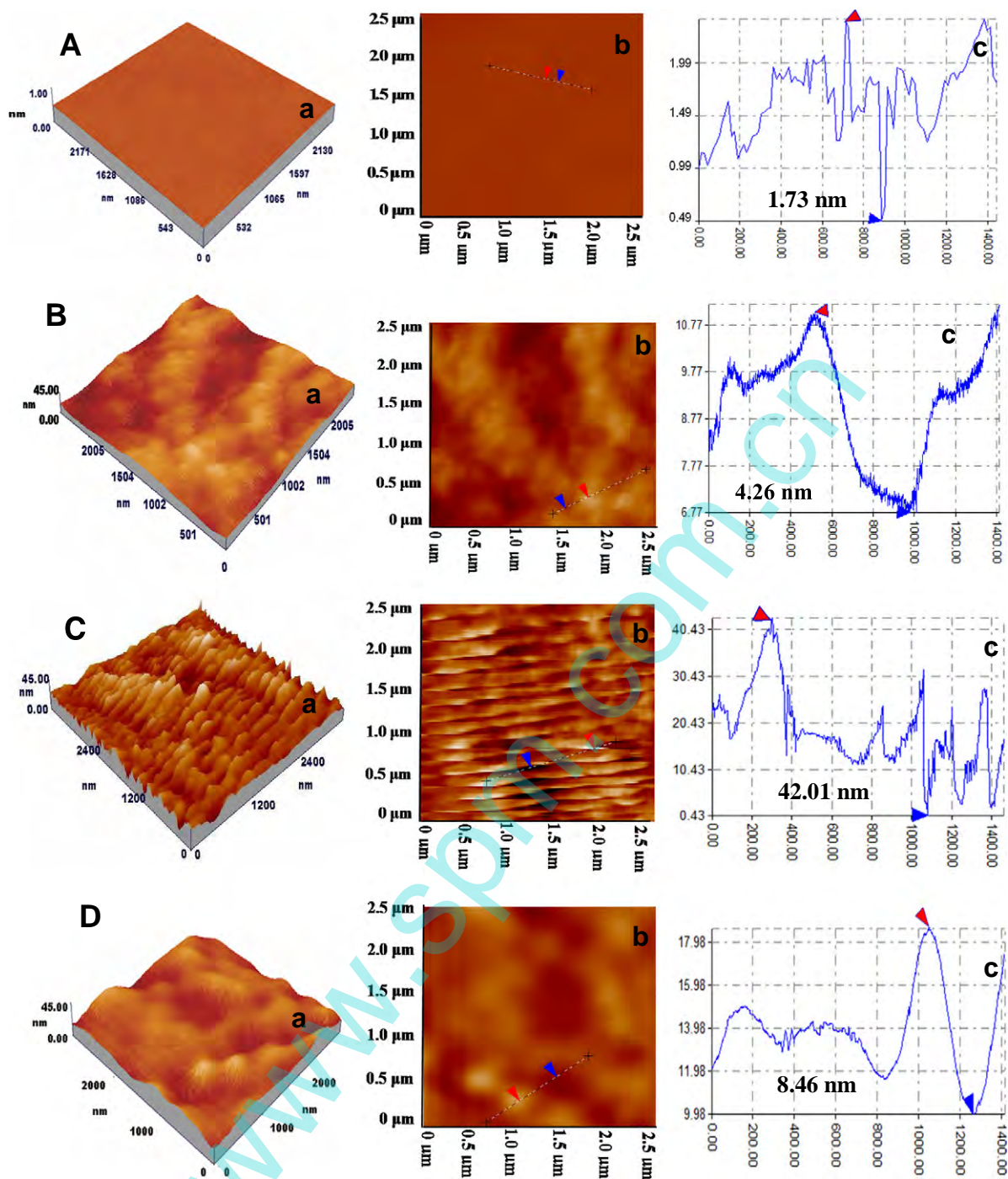
Fig. 2. Three-dimensional (a), topographic (b), and cross-sectional (c) AFM images of GCE (A), GO/GCE (B), PB-GO/GCE (C) and PB-pERGO/GCE (D). The AFM results for PB-GO/GCE and PB-pERGO/GCE were obtained after immersing in Fe^{3+} and $[Fe(CN)_6]^{4-}$ solutions for 10 cycles.

H_2O_2 showed negligible change (Fig. 4A), suggesting that the ERGO alone had no obvious electrocatalytic activity for H_2O_2 reduction. However, on Nafion/PB-GO/GCE (Fig. 4B), it was found that PB still presents good redox peak (curve a), and when H_2O_2 was added into the electrolyte, an increase of 21 μA was observed for the reduction peak, which suggested that the PB in the modified film had the electrocatalytic effect on the reduction of H_2O_2 [36]. It was interesting that when Nafion/PB-ERGO/GCE was applied for determination, the reduction peak of PB increased more significant (85 μA), suggesting that the sensing film of PB/ERGO had higher electrocatalytic ability for the reduction of H_2O_2, due to the fast catalytic electron transfer process of PB on ERGO through

the following equation:

$$2K_2Fe^{II}\left[Fe^{II}(CN)_6\right]+2H_2O_2+4H^+ \xrightarrow{ERGO,-2e} 2KFe^{III}\left[Fe^{II}(CN)_6\right]+4H_2O + 2K^+ \tag{2}$$
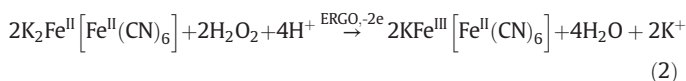
3.4. Amperometric performance of H_2O_2 at Nafion/PB-ERGO/GCE

To further investigate the analytical performance of the sensor, the amperometric curve of Nafion/PB-ERGO/GCE in H_2O_2 solution was
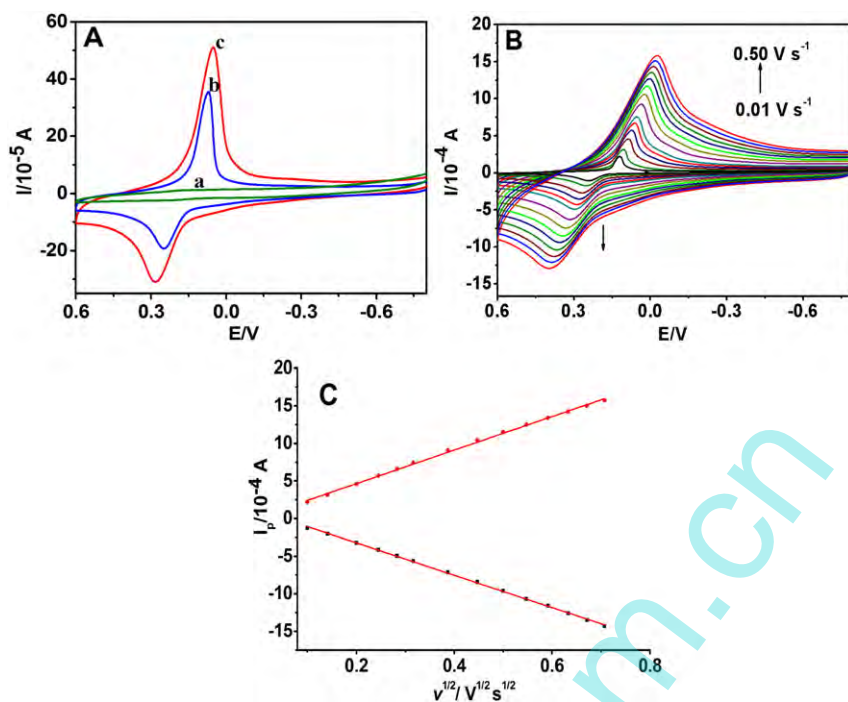
Fig. 3. (A) Cyclic voltammograms (a) GO/GCE, (b) PB-GO/GCE, and (c) PB-ERGO/GCE in 0.1 M KCl (pH = 2.0). (B) Cyclic voltammograms of Nafion/PB-ERGO/GCE with different scan rates (v) in 0.1 M KCl (pH = 2.0) aqueous solution (from inner to outer): 0.01, 0.02, 0.04, 0.06, 0.08, 0.10, 0.15, 0.20, 0.25, 0.30, 0.35, 0.40, 0.45, 0.50 V s^{-1}, respectively. (C) The relationship of cathodic peak current (I_{pc}) and anodic peak current (I_{pa}) versus square root of scan rates ($v^{1/2}$), respectively.

recorded. Fig. 5A showed the typical amperometric response of Nafion/PB-ERGO/GCE at different applied potentials, upon injection of increasing amount of H_2O_2. It was clearly seen that the sensitivity of the amperometric curve changed greatly with the variation of the applied potential, and the largest sensitivity occurred at −0.25 V. Therefore, the applied potential of −0.25 V was selected for the following quantitative analysis.

Fig. 5B showed amperometric responses of Nafion/PB-ERGO/GCE in 0.1 M KCl (pH = 2.0) with successive injection of H_2O_2 under the applied potential of −0.25 V. As shown, obvious increase of catalytic reduction current was observed during successive additions of H_2O_2. Inset of Fig. 5B further revealed that the sensor showed a fast catalytic response toward H_2O_2 reduction, as judged from the fact that the catalytic current reached steady-state within 3 s upon injection of H_2O_2,
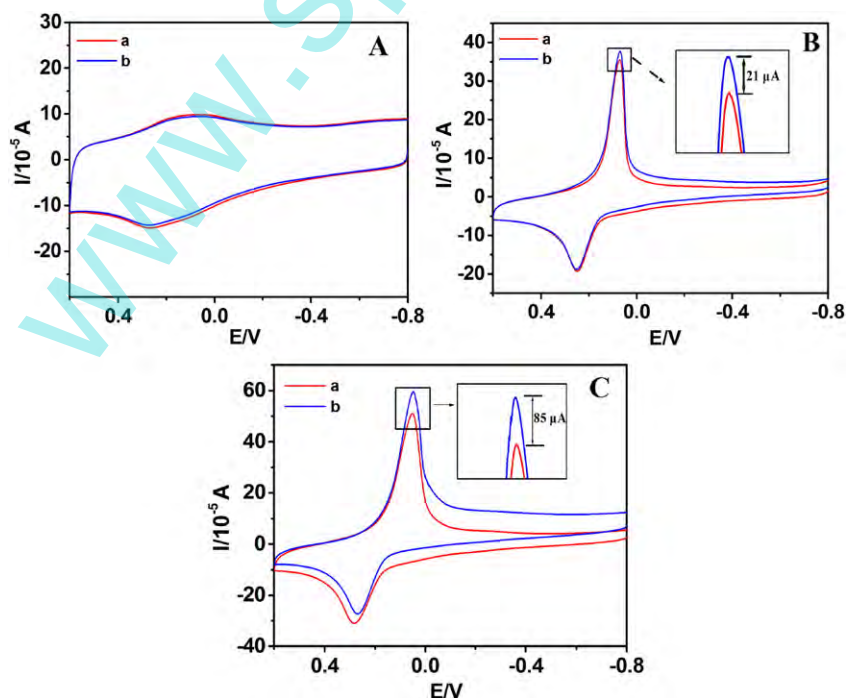
Fig. 4. Cyclic voltammograms of (A) Nafion/ERGO/GCE, (B) Nafion/PB-GO/GCE, (C) Nafion/PB-ERGO/GCE in 0.1 M KCl (pH = 2.0) solution at scan rate of 0.1 V s^{-1} without (a) and with (b) 1.0 mM H_2O_2.
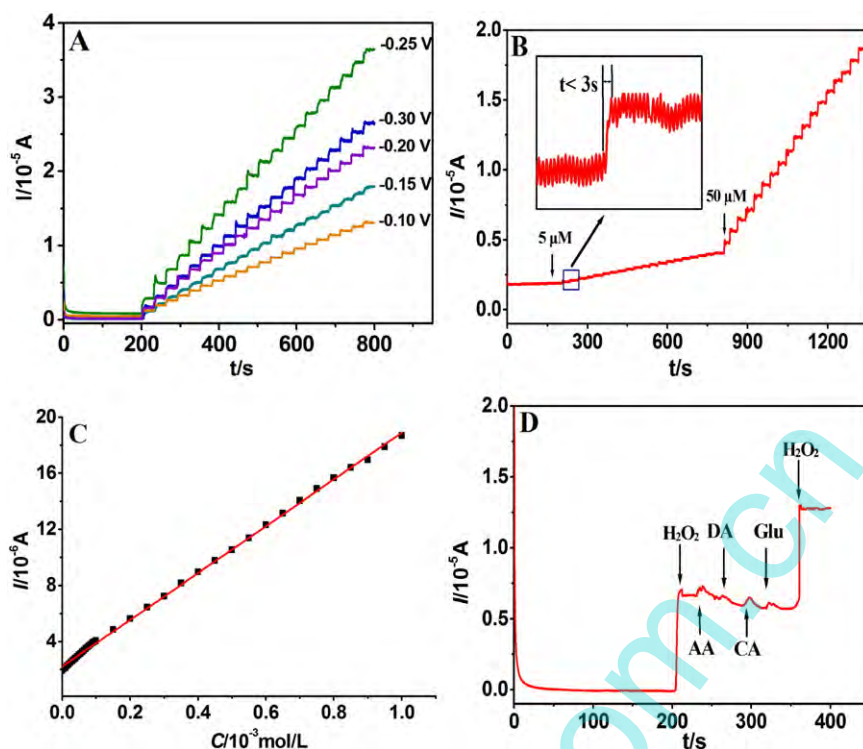
Fig. 5. (A) Amperometric responses of Nafion/PB-ERGO/GCE upon successive injection of 0.1 mM H_2O_2 at different potentials. (B) Amperometric responses of Nafion/PB-ERGO/GCE upon successive additions of H_2O_2 at an applied potential of −0.25 V. Inset: The current response time after addition H_2O_2 at Nafion/PB-ERGO/GCE. (C) Calibration plots of catalytic current (*I*) against H_2O_2 concentrations (*C*). (D) Amperometric response of Nafion/PB-ERGO/GCE to 0.5 mM H_2O_2 in the presence of 0.5 mM AA, DA, UA and glucose.

which was shorter than many reported values in literatures [37–40]. A linear relationship was obtained in the range from 5.0 μM to 1 mM between catalytic currents (*I*) and H_2O_2 concentrations (*C*) (Fig. 5C), with the linear regression equation of I (μA) = $0.02013C_{H2O2}$ (μM) + 2.201 (R = 0.995). Based on a signal-to-noise ratio of 3, the limit of detection was estimated to be 0.8 μM. Although the detection limit of the sensor was slightly higher than some of the other H_2O_2 sensors [27,41,42], the presented method for in-situ preparation of PB material coupled with electrochemical reduced GO layer exhibited the advantages such as low cost, easy operation, high conductivity and fast sensing response.

The influence of some endogenous species, such as AA, DA, UA and Glu on the catalytic response were investigated to evaluate the selectivity of the PB-ERGO-based H_2O_2 sensor. As showed in Fig. 5D, the addition of H_2O_2 (0.5 mM) leads to a dramatic increase in catalytic current. However, the current response showed very small change after the addition of 0.5 mM DA, AA, UA and Glu, respectively. Moreover, the current response remains significant enhancement after further addition

of 0.5 mM H_2O_2 into the solution containing those interference species. This phenomenon confirmed that Nafion/PB-ERGO/GCE could be used as a highly selective sensor for the electrochemical analysis of H_2O_2 in a complex environment.

Furthermore, the stability, reproducibility and repeatability of the sensor were investigated. Fig. 6A showed that the current signal remained 88.7% over a long period of 3600 s. Moreover, the stability of the Nafion/PB-ERGO/GCE was evaluated by storing the prepared sensor at ambient environment, and then electrochemically monitored every 2 days. It was found that 97% of the initial redox peak in CV of the sensor and 91% of the initial catalytic current toward H_2O_2 was retained after 4 weeks, which ascertained its eligible long-term stability (inset, Fig. 6A). The high stability of the sensor could be ascribed to the stable chemical performance of PB material and tight immobilization of sensing platform on electrode surface through the covalent method. Additionally, when six Nafion/PB-ERGO/GCE were fabricated independently under the same conditions and applied for detection of 0.5 mM H_2O_2, a relative standard deviation (RSD) value of 4.8% was
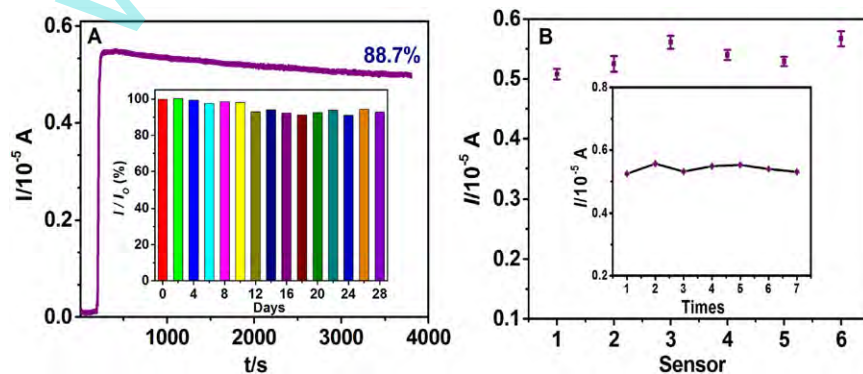
Fig. 6. (A) Amperometric response toward 0.5 mM H_2O_2 over a long time-period of 3600 s. Inset: the stability of the sensor to H_2O_2 tested every two days for 4 weeks. (B) Reproducibility of six Nafion/PB-ERGO electrodes for detection of 0.5 mM H_2O_2. Inset: Repeatability of Nafion/PB-ERGO/GCE for detecting 0.5 mM H_2O_2 seven times.

achieved (Fig. 6B), indicating an acceptable reproducibility of the sensor for analysis application. Repeatability was also measured with one electrode used to detect 0.5 mM H_2O_2 seven times, as shown in inset of Fig. 6B, the RSD of current response was 4.2%. The results showed that the excellent stability, reproducibility and repeatability of the Nafion/PB-ERGO/GCE were reliable for H_2O_2 sensing.

3.5. Detection of H_2O_2 released from living macrophages

In order to validate the practical application of Nafion/PB-ERGO/GCE for measurement of H_2O_2 released from living cells. Macrophages, the chemotactically responsive cells, play an important role in host defense against various microbes as well as tumors [43]. So, we used macrophages as cell example and used Lipopolysaccharide (LPS) to stimulate H_2O_2 generation of the cells. As shown in Fig. 7, in a blank electrolyte solution without macrophages, no obvious current change was observed when LPS was added (curve a). Nevertheless, when LPS was added into the electrolyte in the presence of 6.4×10^6 macrophages, the catalytic current increased rapidly (curve b), showing that H_2O_2 had been generated from living cells. Then the injection of 300 unit mL^{-1} catalase, the current decreased again. This is because catalase was a selective enzyme for the decomposition of H_2O_2. According to the current change (4.5 μA) for these cells, the H_2O_2 released from each cell was calculated to be about 1.83×10^{-14} mol, which agrees well with the earlier literatures [44,45], showing that our developed sensor was feasible to real-time monitor the H_2O_2 released from living cells.

4. Conclusions

In this paper, covalent bonding method was applied for immobilization of GO on an oxidized glassy carbon electrode, which was further utilized as a supporting platform for the in-situ synthesis of PB. Characterization experiments suggested that the rich oxygen-containing groups play a crucial role for the growth of PB. Furthermore, GO in the PB-GO film was reduced to ERGO through an environmentally friendly and effective electrochemical reduced method. Such a protocol for the fabrication of PB-based modified electrode has advantages: (1) The morphology and growing amount of PB could be well controlled by turning the dipping circles of the electrode in Fe^{3+} and $[Fe(CN)_6]^{4-}$ solutions. (2) The stability of the modified film can be greatly improved by the combination of in-situ synthesis of PB covalent immobilization of GO and electrochemical reduction of GO. Based on these advantages, when Nafion/PB-ERGO/GCE was applied for the H_2O_2 detection through amperometry, fast response rate, high current response and wide dynamic range were achieved. In addition, when the developed sensor was applied for real-time detection of H_2O_2 released from living cells, and satisfactory results were obtained. The present work provided us

a new strategy for the fabrication of non-enzymatic electrochemical sensor for H_2O_2 in biological samples.

References

[1] L. Fu, Y.H. Zheng, A.W. Wang, W. Cai, Z.X. Fu, F. Peng, A novel nonenzymatic hydrogen peroxide electrochemical sensor based on SnO$_2$-reduced graphene oxide nanocomposite, Sens. Lett. 13 (2015) 81–84.
[2] R.G. Cutler, S. Camandola, K.F. Malott, M.A. Edelhauser, M.P. Mattson, The role of uric acid and methyl derivatives in the prevention of age-related neurodegenerative disorders, Curr. Top. Med. Chem. 15 (2015) 2233–2238.
[3] M. Tomczynska, M. Bijak, J. Saluk, Metformin-the drug for the treatment of autoimmune diseases; a new use of a known anti-diabetic drug, Curr. Top. Med. Chem. 16 (2016) 2223–2230.
[4] T.K. Ryan, W.Y. Jacky, B. ZhongáTang, An AIE-active fluorescence turn-on bioprobe mediated by hydrogen-bonding interaction for highly sensitive detection of hydrogen peroxide and glucose, Chem. Commun. 52 (2016) 10076–10079.
[5] J. Ju, W. Chen, In situ growth of surfactant-free gold nanoparticles on nitrogen-doped graphene quantum dots for electrochemical detection of hydrogen peroxide in biological environments, Anal. Chem. 87 (2015) 1903–1910.
[6] L. Wang, S.H. Ma, B. Yang, W.W. Cao, X.J. Han, Morphology-controlled synthesis of Ag nanoparticle decorated poly (o-phenylenediamine) using microfluidics and its application for hydrogen peroxide detection, Chem. Eng. J. 268 (2015) 102–108.
[7] P. Kanyong, S. Rawlinson, J. Davis, A non-enzymatic sensor based on the redox of ferrocene carboxylic acid on ionic liquid film-modified screen-printed graphite electrode for the analysis of hydrogen peroxide residues in milk, J. Electroanal. Chem. 766 (2016) 147–151.
[8] N. Akhtar, S.A. El-Safty, M. Khairy, W.A. El-Said, Fabrication of a highly selective non-enzymatic amperometric sensor for hydrogen peroxide based on nickel foam/cytochrome c modified electrode, Sensors Actuators B Chem. 207 (2015) 158–166.
[9] Y.P. Lin, X. Chen, Y.X. Lin, Q. Zhou, D.P. Tang, Non-enzymatic sensing of hydrogen peroxide using a glassy carbon electrode modified with a nanocomposite made from carbon nanotubes and molybdenum disulfide, Microchim. Acta 182 (2015) 1803–1809.
[10] Y.L. Wang, Z.C. Wang, Y.P. Rui, M.G. Li, Horseradish peroxidase immobilization on carbon nanodots/CoFe layered double hydroxides: direct electrochemistry and hydrogen peroxide sensing, Biosens. Bioelectron. 64 (2015) 57–62.
[11] Y.Q. Yang, H.L. Xie, J. Tang, S. Tang, J. Yi, H.L. Zhang, Design and preparation of a nonenzymatic hydrogen peroxide sensor based on a novel rigid chain liquid crystalline polymer/reduced graphene oxide composite, RSC Adv. 5 (2015) 63662–63668.
[12] J. Anojčić, V. Guzsvány, O. Vajdle, D. Madarász, A. Rónavári, Z. Kónya, K. Kalcher, Hydrodynamic chronoamperometric determination of hydrogen peroxide using carbon paste electrodes coated by multiwalled carbon nanotubes decorated with MnO$_2$ or Pt particles, Sensors Actuators B Chem. 233 (2016) 83–92.
[13] L.L. Zhang, Y.J. Han, J.B. Zhu, Y.L. Zhai, S.J. Dong, Simple and sensitive fluorescent and electrochemical trinitrotoluene sensors based on aqueous carbon dots, Anal. Chem. 87 (2015) 2033–2036.
[14] E.N. Afshar, R. Rouhi, N.E. Gorji, Review on the degradation and device physics of quantum dot solar cells, Mod. Phys. Lett. B 29 (2015) 1530008.
[15] A. Mebadi, M. Houshmand, M.H. Zandi, N.E. Gorji, Simulations of the intermediate bandwidth fluctuations in nanostructured PV, Physica E 53 (1) (2013) 130–136.
[16] J. Zhang, J.L. He, W.L. Xu, L.L. Gao, Y.L. Guo, W.J. Li, C. Yu, A novel immunosensor for detection of beta-galactoside alpha-2, 6-sialyltransferase in serum based on gold nanoparticles loaded on Prussian blue-based hybrid nanocomposite film, Electrochim. Acta 156 (2015) 45–52.
[17] S. Cinti, F. Arduini, D. Moscone, G. Palleschi, L. Gonzalez-Macia, A.J. Killard, Cholesterol biosensor based on inkjet-printed Prussian blue nanoparticle-modified screen-printed electrodes, Sensors Actuators B Chem. 221 (2015) 187–190.
[18] G.S. Lai, H.L. Zhang, A.M. Yu, H.X. Ju, In situ deposition of Prussian blue on mesoporous carbon nanosphere for sensitive electrochemical immunoassay, Biosens. Bioelectron. 74 (2015) 660–665.
[19] P.C. Pandey, D. Panday, Tetrahydrofuran and hydrogen peroxide mediated conversion of potassium hexacyanoferrate into Prussian blue nanoparticles: application to hydrogen peroxide sensing, Electrochim. Acta 190 (2016) 758–765.
[20] Q.L. Sheng, D. Zhang, Q. Wu, J.B. Zheng, H.S. Tang, Electrodeposition of Prussian blue nanoparticles on polyaniline coated halloysite nanotubes for nonenzymatic hydrogen peroxide sensing, Anal. Methods 7 (2015) 6896–6903.
[21] L. Chao, W. Wang, M.Z. Dai, Y.X. Ma, L.G. Sun, X.L. Qin, Q.J. Xie, Step-by-step electrodeposition of a high-performance Prussian blue-gold nanocomposite for H_2O_2 sensing and glucose biosensing, J. Electroanal. Chem. 778 (2016) 66–73.
[22] X. Zhu, X.H. Niu, H.L. Zhao, M.B. Lan, Doping ionic liquid into Prussian blue-multiwalled carbon nanotubes modified screen-printed electrode to enhance the nonenzymatic H_2O_2 sensing performance, Sensors Actuators B Chem. 195 (2014) 274–280.

Fig. 7. Amperometric responses of Nafion/PB-ERGO/GCE in 0.1 M KCl (pH = 2.0) with the addition of 8 μg ml^{-1} LPS in the absence (a) and presence (b) of macrophages.

[23] R.C. Millward, C.E. Madden, I. Sutherland, R.J. Mortimer, S. Fletcher, F. Marken, Directed assembly of multilayers—the case of Prussian blue, Chem. Commun. 19 (2001) 1994–1995.

[24] S. Manivannan, I. Kang, K. Kim, In situ growth of Prussian blue nanostructures at reduced graphene oxide as a modified platinum electrode for synergistic methanol oxidation, Langmuir 32 (2016) 1890–1898.

[25] R. Ojani, P. Hamidi, J.B. Raoof, Efficient nonenzymatic hydrogen peroxide sensor in acidic media based on Prussian blue nanoparticles-modified poly (o-phenylenediamine)/glassy carbon electrode, Chin. Chem. Lett. 27 (2016) 481–486.

[26] S. Pei, H.M. Cheng, The reduction of graphene oxide, Carbon 50 (2012) 3210–3228.

[27] J.H. Yang, N. Myoung, H.G. Hong, Facile and controllable synthesis of Prussian blue on chitosan-functionalized graphene nanosheets for the electrochemical detection of hydrogen peroxide, Electrochim. Acta 81 (2012) 37–43.

[28] W.S. Hummers, R.E. Offeman, Preparation of graphitic oxide, J. Am. Chem. Soc. 80 (1958) 1339.

[29] F. Li, J.X. Song, C.S. Shan, D.M. Gao, X.Y. Xu, L. Niu, Electrochemical determination of morphine at ordered mesoporous carbon modified glassy carbon electrode, Biosens. Bioelectron. 25 (2010) 1408–1413.

[30] X. Wang, Q.X. Wang, Q.H. Wang, F. Gao, F. Gao, Y.Z. Yang, H.X. Guo, Highly dispersible and stable copper terephthalate metal–organic framework–graphene oxide nanocomposite for an electrochemical sensing application, ACS Appl. Mater. Interfaces 6 (2014) 11573–11580.

[31] J. Ventura, S.J. Eron, D.C. González-Toro, K. Raghupathi, F. Wang, J.A. Hardy, S. Thayumanavan, Reactive self-assembly of polymers and proteins to reversibly silence a killer protein, Biomacromolecules 16 (2015) 3161–3171.

[32] R.A. Burga, S. Patel, C.M. Bollard, C.R. Y Cruz, R. Fernandes, conjugating Prussian blue nanoparticles onto antigen-specific T cells as a combined nanoimmunotherapy, Nanomedicine 11 (2016) (1759-1767).

[33] S. Husmann, A.J.G. Zarbin, Design of a Prussian blue analogue/carbon nanotube thin-film nanocomposite: tailored precursor preparation, synthesis, characterization, and application, Chem. Eur. J. 22 (2016) 6643–6653.

[34] Y.J. Zou, Q.Y. Wang, C.L. Xiang, Z. She, H.L. Chu, S.J. Qiu, L.X. Sun, One-pot synthesis of ternary polypyrrole–Prussian-blue–graphene-oxide hybrid composite as electrode material for high-performance supercapacitors, Electrochim. Acta 188 (2016) 126–134.

[35] M.V. Mirkin, H.J. Yang, A.J. Bard, Borohydride oxidation at a gold electrode, J. Electrochem. Soc. 139 (1992) 2212–2217.

[36] M.M. Liu, R. Liu, W. Chen, Graphene wrapped Cu_2O nanocubes: non-enzymatic electrochemical sensors for the detection of glucose and hydrogen peroxide with enhanced stability, Biosens. Bioelectron. 45 (2013) 206–212.

[37] H. Kivrak, O. Alal, D. Atbas, Efficient and rapid microwave-assisted route to synthesize Pt–MnO_x hydrogen peroxide sensor, Electrochim. Acta 176 (2015) 497–503.

[38] J.C. Li, Y.Z. Jiang, Y.Y. Zhai, H.Q. Liu, L. Li, Prussian blue/reduced graphene oxide composite for the amperometric determination of dopamine and hydrogen peroxide, Anal. Lett. 48 (2015) 2786–2798.

[39] X. Qin, H.C. Wang, Z.Y. Miao, J.L. Li, Q. Chen, A novel non-enzyme hydrogen peroxide sensor based on catalytic reduction property of silver nanowires, Talanta 139 (2015) 56–61.

[40] Y.Y. Zhang, C. Zhang, D. Zhang, M. Ma, W.Z. Wang, Q. Chen, Nano-assemblies consisting of Pd/Pt nanodendrites and poly (diallyldimethylammonium chloride)-coated reduced graphene oxide on glassy carbon electrode for hydrogen peroxide sensors, Mater. Sci. Eng. C 58 (2016) 1246–1254.

[41] Z.D. Xu, L.Z. Yang, C.L. Xu, Pt@UiO-66 heterostructures for highly selective detection of hydrogen peroxide with an extended linear range, Anal. Chem. 87 (2015) 3438–3444.

[42] J.F. Huang, Y.H. Zhu, H. Zhong, X.L. Yang, C.Z. Li, Dispersed CuO nanoparticles on a silicon nanowire for improved performance of nonenzymatic H_2O_2 detection, ACS Appl. Mater. Interfaces 6 (2014) 7055–7062.

[43] S. Dong, J.B. Xi, Y.N. Wu, H.W. Liu, C.Y. Fu, H.F. Liu, F. Xiao, High loading MnO_2 nanowires on graphene paper: facile electrochemical synthesis and use as flexible electrode for tracking hydrogen peroxide secretion in live cells, Electrochim. Acta 853 (2015) 200–206.

[44] W.L. Qiu, M.Z. Xu, R.X. Li, X.M. Liu, M.N. Zhang, Renewable and ultralong nanoelectrochemical sensor: nanoskiving fabrication and application for monitoring cell release, Anal. Chem. 88 (2015) 1117–1122.

[45] Z.Z. Li, Y.M. Xin, Z.H. Zhang, New photocathodic analysis platform with quasi-core/shell-structured TiO_2@Cu_2O for sensitive detection of H_2O_2 release from living cells, Anal. Chem. 87 (2015) 10491–10497.